


PSFC/JA-00-35

Core Internal Transport Barriers on Alcator C-Mod

View metadata, citation and similar papers at core.ac.uk

brought to you by  C
provided by DSpace

E.S. Marmor, D. Mossessian, M. Porkolab, G. Taylor¹,
J. Snipes, S.M. Wolfe, S.J. Wukitch

October 2000

Plasma Science and Fusion Center
Massachusetts Institute of Technology
Cambridge, MA 02139 USA

¹Princeton Plasma Physics Laboratory, Princeton, NJ.

This work was supported by the U.S. Department of Energy, Cooperative Grant No. DE-FC02-99ER54512. Reproduction, translation, publication, use and disposal, in whole or in part, by or for the United States government is permitted.

Submitted for publication to *Physics of Plasmas*.

Core internal transport barriers on Alcator C-Mod

C.L. Fiore, J. E. Rice, P.T. Bonoli, R. L. Boivin, J. A. Goetz, A. E. Hubbard, I. H.

Hutchinson, R. S. Granetz, M. J. Greenwald, E. S. Marmor, D. Mossessian, M. Porkolab, G.

Taylor*, J. Snipes, S. M. Wolfe, S. J. Wukitch

Plasma Science and Fusion Center, Massachusetts Institute of Technology, Cambridge,

Massachusetts 02139

*Princeton Plasma Physics Laboratory, Princeton, New Jersey

Abstract

The formation of internal transport barriers (ITB) has been observed in the core region of Alcator C-Mod under a variety of conditions. The improvement in core confinement following pellet injection (pellet enhanced performance or PEP mode) has been well documented on Alcator C-Mod in the past. Recently three new ITB phenomena have been observed which require no externally applied particle or momentum input. Short lived ITBs form spontaneously following the high confinement (H) to low confinement (L) mode transition and are characterized by a large increase in the global neutron production (enhanced neutron or EN modes.) Experiments with ICRF (ion cyclotron range of frequencies) power injection to the plasma off-axis on the high field side results in the central density rising abruptly and becoming peaked. The ITB formed at this time lasts for 10 energy confinement times. The central toroidal rotation velocity decreases and changes sign as the density rises. Similar spontaneous ITBs have been observed in

ohmically heated H-mode plasmas. All of these ITB events have strongly peaked density profiles with a minimum in the density scale length occurring near $r/a = 0.5$ and have improved confinement parameters in the core region of the plasma.

Catherine L. Fiore, MIT NW21-203, 77 Mass. Ave. Cambridge, MA 02139
Fiore@psfc.mit.edu

I. Introduction

The observation of transport barriers in tokamak plasmas has been well documented, especially at the edge of the plasma during H-mode in most divertor style tokamaks.^{1,2}

Transport barriers in the core plasma region were first reported following the injection of frozen hydrogen pellets into the Alcator C tokamak³ and have since been observed with lithium pellet injection as well.⁴ A number of experiments have reported core internal transport barriers (ITB's) while using high power neutral beam injection and control of the shear profile in the plasma,^{5,6,7,8,9} which, like pellet injection, provides a particle source in the center of the plasma.

Core transport barriers have been noted with electron cyclotron heating (ECRH)¹⁰, ion Bernstein wave injection (IBW)¹¹ and lower hybrid heating (LHH)¹² when the device is operated in a manner to cause a region of reverse magnetic shear to form in the plasma. These internal transport barrier regions are notable in that an area of reduced transport in one or more of the thermal, particle, or momentum channels for either the ions or the electrons is bounded by a region of strong plasma density gradient.¹³

Internal transport barriers have been observed for a variety of operational parameters in Alcator C-Mod plasmas. Most notably they have been seen with the injection of lithium pellets¹⁴ and have been reported in cases where extreme reverse shear is generated in conjunction with ICRF (ion cyclotron range of frequencies) heating.¹⁵

Recent experiments in Alcator C-Mod have produced plasmas with improved confinement and marked internal transport barriers within the core region of the plasma, the barriers forming at $0.3 < r/a < 0.5$. Most remarkably, these arise without the addition of external particle or momentum sources. Three distinct new phenomena have been observed. First, during the high confinement (H) mode to low confinement (L) mode back transition the electron density becomes significantly peaked and the global neutron rate increases sharply. Eightfold increases in the neutron production have been seen, leading this event to be called the enhanced neutron mode (EN). These events occur frequently but are short lived, lasting less than 50 ms, or about 1 energy confinement time. Secondly, when using ICRF power injection to the plasma with the resonance for the hydrogen minority absorption (deuterium majority) off-axis on the high field side, it has been observed that the central density rises abruptly and becomes peaked; the ITB formed at this time lasts for 10 or more energy confinement times. The central toroidal plasma rotation slows and even reverses sign at the same time. Finally, the spontaneous formation of peaked density profiles and improved confinement concurrent with the decline in plasma rotation has been observed in ohmic H-mode plasmas as well. These events occur with no internal source of fueling to the plasma core. The experimental details will be presented here,

and compared to those for the previously reported pellet enhanced performance (PEP mode) plasmas.

II. Experimental Description and Diagnostics

The Alcator C-Mod tokamak is a compact (major radius $R=0.67$ m, minor radius $a=0.22$ m), high field device ($2.6 < B_t < 8.1$ T). The operating range includes plasma current up to 1.5 MA, and gas fueled average density up to $5.9 \times 10^{20} \text{ m}^{-3}$. Normal operation uses a lower single null with closed divertor. The walls are molybdenum tiles that are coated with boron frequently during run campaigns. Currently the only available heating source other than ohmic power is 80 MHz ICRF heating. Up to 8MW of ICRF source power can be delivered through 3 antennas: 2 two-strap units, and 1 four-strap antenna.

H-mode plasmas have been obtained under a wide range of conditions in Alcator C-Mod, spanning the full operational range of the device, with line averaged density up to $4.8 \times 10^{20} \text{ m}^{-3}$. H-modes are routinely seen in both purely ohmic heated discharges as well as during ICRF powered plasmas. The edge localized modes (ELMs)¹⁶ seen on other devices seldom appear during H-modes in Alcator C-Mod. The bulk of H-Mode plasmas are either ELM-free or exhibit enhanced D_α emission (EDA).¹⁷

Alcator C-Mod is equipped with an extensive set of standard core diagnostics. The results reported here use data from the following systems. Electron temperature profiles are

obtained from two grating polychromator electron cyclotron emission diagnostics, one with 9 and the other with 18 spatial channels.¹⁸ Density profiles are obtained from multichord interferometry, Thomson scattering, and from a CCD based one-dimensional imaging system measuring visible bremsstrahlung emission from the plasma.¹⁹ While taking account of Z_{eff} , assumed to be flat across the profile, as is typical for Alcator C-Mod plasmas, and also accounting for a weak electron temperature dependence, the square root of the emission profile will be the same as the electron density profile. A limited amount of ion temperature profile data is obtained from a scannable array of 5 high spectral resolution x-ray spectrometers (HIREX).²⁰ In addition, measurements of central toroidal plasma rotation are obtained from x-ray spectra recorded by a spatially fixed tangentially viewing von Hamos type crystal x-ray spectrometer²¹ and confirmed independently from frequency analysis of sawtooth pre- and post-cursors.²²

The total neutron flux is measured using two different systems. The first consists of 18 different neutron detectors of different types and sensitivities, a mix of fission chambers, boron-trifluoride filled proportional counters, and He^3 filled detectors.²³ These are distributed among 4 moderator filled cans at different locations in the Alcator C-Mod cell. Two of these are absolutely calibrated with Cf^{252} , and the others are cross-calibrated from these using the d-d fusion neutrons from Alcator C-Mod. The arrangement provides good dynamic range, but the time resolution is limited to 1 ms because they are operated in count rate mode. The second detector system is made up of 14 He^3 filled proportional counters surrounded by polyethylene moderator. Their outputs are connected in parallel, producing a small current proportional to the

impinging neutron flux. Measurement of this current can be done with time resolution of 0.1 ms, and is limited only by the slowing-down time of the thermonuclear neutrons in the moderator. Sawtooth oscillations can clearly be seen in the output of this system. The magnitude of the output is scaled to that from the absolutely calibrated system to provide a fast measurement of the total neutron production from Alcator C-Mod.

III. Observation of Alcator C-Mod Internal Transport Barriers

All occurrences of internal transport barriers on Alcator C-Mod are marked by the peaking of the electron density profiles. While the plasma temperatures typically increase during these events, a similar narrowing of the temperature profiles is not seen. Density profiles from the different types of ITBs found in Alcator C-Mod are shown in Fig. 1. The profile evolution shown in Fig. 1.a) is characteristic of the enhanced neutron (EN) mode, a short lived ITB event which occurs shortly after the plasma makes a transition from H- to L-mode. The usually flat density profile which includes the typical H-mode edge pedestal is shown immediately prior to the transition. In short order, the density collapses in the outer region of the plasma while the central value is unchanged, temporarily resulting in a strongly peaked radial distribution. While the density is peaked, the neutron production rate increases sharply, persisting through several sawtooth cycles until the central density collapses and the plasma has fully achieved L-mode.

The entire sequence lasts approximately 50 ms, the neutron rate increase lasting about 1 energy confinement time.

In contrast, the density profile evolution of the pellet enhanced performance (PEP) mode is shown in Fig. 1.b). The lowest density value is the profile just before the lithium pellet is fired into the plasma, and the highest is shortly after the pellet. The ICRF heating is turned on after the ITB has formed, 2 ms before the highest profile shown at a power of 3 MW. The profiles decrease in magnitude and return to pre-pellet levels 110 ms after the pellet is fired. The neutron rate reaches its peak value 101 ms after the pellet injection, by which time the central density has decreased substantially from its peak level. The internal poloidal magnetic field has been measured during lithium pellet PEP mode on Alcator C-Mod by imaging the pellet ablation trail,¹⁴ and it was demonstrated that the current density profile following the pellet was hollow, resulting in a region of reverse shear in the plasma core.

Internal transport barriers have also been observed with off-axis ICRF injection. The profile evolution, shown in Fig 1.c, starts just as the central density begins to rise. The core density continues to increase steadily over the next 300 ms, finally collapsing as the central radiated power becomes large due to impurity accumulation in the core. An H-mode edge is maintained throughout. The core density increase is remarkable in that no central fueling source is available in either this case or in that shown in Fig. 1d, a peaked density ohmic H-mode plasma. The peaked density shown here arose spontaneously after the plasma went into H-mode. The ohmic H-mode is typically induced by ramping the toroidal magnetic field down to a low

value, and the plasma sawtooth activity slows and stops while the density is most peaked suggesting that q_0 exceeds 1 for at least part of this event. In this case the core ITB lasted more than 400 ms, at least 10 energy confinement times, ending only as the plasma current began to ramp down in a controlled termination of the discharge.

Remarkably, in the case of the ITBs which are seen with off-axis ICRF and in peaked ohmic H-modes, the co-current plasma rotation, that has been well documented to occur in all high pressure Alcator C-mod plasmas²¹ is seen to slow and even slightly reverse itself as the central density begins to rise. An example of the rotation velocity is compared for two similar discharges in Fig 2. In both cases ICRF power of 3 MW is turned on at $t = 0.7$ s, and the plasma enters into H-mode almost immediately. In the case represented by the dashed line, the toroidal field was 4.9 T and the rf resonant layer was slightly off-axis on the high field side ($r/a=0.25$). The ratio of central electron density to that from one of the outer channels ($r/a=0.73$) from the same shot shows no peaking throughout the H-mode phase of the plasma. The solid trace in both figures is from a plasma with the same conditions, except that the toroidal field was at 4.5 T, bringing the rf resonance layer to $r/a=0.5$, in the region where the ITB is typically located in the Alcator C-Mod core. As can be easily seen, the rotation started to rise when the ICRF power was turned on at 0.7 s, and then it began to decrease monotonically 0.2 s later. Shortly thereafter, the density peaking factor has begun to increase, and it is clear that an ITB has formed, as is shown by the ratio of central to outer electron density for that same shot and in the profiles shown in Fig. 1.c). By considering neoclassical momentum and heat balance, the

internal radial electric field is inferred to start from an initial value of 12 kV/m at $r/a=0.33$ and to reverse sign, ultimately reaching -18 kV/m.²³

IV. Enhanced Neutron (EN) Mode ITB

The ITB which is formed at the H to L-mode transition in Alcator C-Mod is characterized by a large spike on the global neutron production. This increase typically lasts 3 or fewer sawtooth cycles, about 30 to 40 ms, or approximately 1 energy confinement time. The size of the neutron rate increase relative to the preceding H-mode value can be as little as 30%, although factors of 2 to 8 are common. EN mode is seen following the majority of H-to L-mode transitions, in both ICRF and Ohmic plasmas. The fact that these events occur frequently and predictably, and that they can be induced at will, means that they can be studied in a systematic manner, and that parametric characterization is possible.

Data from a typical Alcator C-Mod H- to L-mode transition are shown in Fig. 3. Note that the global neutron rate, shown in the top trace, increases sharply following the transition. The corresponding ion temperature calculated from the neutron rate is shown in the second trace, and shows an increase at the transition as well. The electron temperature is included for comparison. As is typical for Alcator C-Mod H-mode plasmas, the line average density is seen to increase up until the large D_α increase which signals the end of the H-mode period, then it decreases until the plasma returns to H-mode. The ratio of the central density to the density at $r/a=0.73$ obtained from profiles of visible bremsstrahlung radiation shows a marked peaking of

the density, which is also confirmed by Thomson scattering measurements. This is not a result of an increase in either the central density or of the central impurities, but of a marked collapse of the density in the outer part of the plasma. In fact, the density in the center typically shows little or no change until it collapses into a typical L-mode profile. This particular case was heated with 1 MW rf power. The mode seems to decay as the sawteeth redistribute the core particles to the outer part of the plasma, eventually flattening the density profile (typical sawtooth inversion radius is at $r/a=0.25$). The plasma stored energy (not pictured) decreases because of the loss of particles from the outer part of the plasma where the volume is large.

The ratio r/L_n , where L_n is defined as $(1/n_e |dn_e/dr|)^{-1}$ is plotted in Fig. 4 for one such H to L transition in the part of the core region where the density gradient is steepest, $r/a=0.4$. Comparison with the neutron production rate shows a correspondence between the local maximum of r/L_n and the peak neutron rate. In addition, calculation of L_n for a large number of events demonstrates that its minimum value, indicating the steepest point in the core density gradient, occurs at a position $0.3 < r/a < 0.5$ for most of the data studied.

Ion temperature profile data on Alcator C-mod are typically obtained with 0.1 s time resolution which is not sufficient to resolve these short lived core barrier effects. However, by purposely triggering H- to L-mode transitions in similar discharges and averaging data for several pulses, the ion temperature profiles shown in Fig. 5 were obtained with 0.02 s resolution. While the central ion temperature is notably higher following end of the H-mode, the profile is not noticeably more peaked than the profile obtained in the H-mode phase. Gaussian fits to the

data are included in the figure, and the $1/e$ width shows no significant change. The electron temperature profiles are included for comparison, and the width of the T_e Gaussian profiles do not change either. Calculation of the quantity $L_T = [d \ln (T_e) / dr]^{-1}$ for a large number of these transitions shows no change in that quantity, other than that which can be attributed to sawtooth oscillations.

The absence of change in the temperature profiles indicates that variation of the scale length ratio η_x (defined as $d \ln T_x / d \ln n_x$) is determined entirely by changes in the inverse density scale length. There are not sufficient ion temperature profile data to determine η_i for these events, but η_e can be easily obtained. Because of the high density operation in Alcator C-Mod T_e and T_i are equal within experimental error, and η_e is used for an η_i surrogate. As can be seen from Fig. (6.a), η_e at $r/a = 0.5$ decreases significantly during the H to L mode transition, again reaching a minimum value between 1 and 2 near the time that the neutron rate peaks.

In an effort to explore the role of η_e in these spontaneous internal transport barriers, η_e was calculated at the H to L mode transition for many events which showed the characteristic ITB formation. The results, shown in a histogram in Fig. (6.b) demonstrate that η_e consistently drops to a value less than 2 during these transitions.

V. Extended lifetime ITB and transport parameters

As explained earlier, the ITBs which form immediately following the H- to L-mode transition are transient and the density profile relaxes within a few sawtooth cycles, about 40 ms.

It was noted, however, that under plasma conditions where the plasma sawteeth were nearly eliminated that the mode lifetime could be extended for several energy confinement times, especially with off-axis ICRF heating. This has been demonstrated with ICRF injection on the high field side of the plasma in the ITB's formed at the H- to L-Mode transition, and has given rise to ITB formation even in the H-mode phase of the plasma.

It has also been noted that ITBs sometimes form spontaneously in Ohmic H-mode operation (Fig. 1.d) and that the ITB which is formed at the H- to L-mode transition under these conditions can be quite long lived as well. As shown in Fig. 7, the H-mode phase of the plasma, which can be seen from the increasing line average density, ends at 1.09s. At this time the neutron rate doubles, and the density peaking rises to 2.5. The central toroidal rotation begins to decline somewhat before the end of the H-mode, and the effective thermal diffusivity, χ_{eff} , (at $r/a=0.2$), begins to decrease at the same time, reaching neoclassical value during the time when the neutron rate and the density peaking factor are the highest. Radial profiles of the energy confinement time, effective thermal diffusivity, and the plasma bootstrap current density (from TRANSP²⁵ computer code calculations) show that the improvement is in the plasma core, with the bootstrap current peaking at the location of the ITB, at $r/a=0.4$ (Fig. 8). Similar results are found using TRANSP to determine internal transport behavior for the ITB formed during the H- to L-mode transition, with a doubling of the confinement time being typical. A bootstrap current density representing 10% of the total local current density is typically found at the barrier location.

VI. Discussion

The core ITBs observed in Alcator C-Mod all have strongly peaked density profiles with the barrier typically forming at $0.3 < r/a < 0.5$, well outside the sawtooth inversion radius at $r/a=0.25$. No evidence of a barrier is seen in the electron or ion temperature profiles to date. The observation that η_e (and presumably η_i) decreases to the order of 1 in the transport barrier region is suggestive that a suppression of the growth rate for ion temperature gradient driven instabilities could have a role in the improved energy confinement in the core during these events. In addition, the measurements of changes in the central toroidal rotation velocity for the longer lived ITBs indicate that the internal electric field could also be playing a role in suppressing turbulent growth through changing the E X B shearing rate, as has been demonstrated in other devices^{8,26}. However, at this time there has been no measurement of core turbulence in Alcator C-Mod. It is expected that both core turbulence measurements and internal poloidal magnetic field measurements together with detailed ion temperature profiles will be available shortly to help sort out the roles of competing mechanisms.

Several experiments are planned with rf heating to further explore the ITB phenomena on Alcator C-Mod. Dual frequency ICRF power will be available to both heat the plasma center while at the same time heating off-axis to trigger the ITB. In a different scenario, ion Bernstein waves will be used to drive current and tailor the poloidal magnetic field in order to study ITB

control with reverse-shear. And finally, lower hybrid current drive is planned to control the current density profile and form ITBs while ICRF power is used to add heat to the plasma core.

VII. Acknowledgements

This work is support by D.o.E. Coop. Agreement DE-FC02-99ER54512. The authors would like to thank Bill Rowan for useful discussions, and Jim Irby, Dave Gwinn, and the Alcator C-Mod engineering and technical staff for providing regular and reliable experimental operation.

References

- ¹I. H. Hutchinson, R. S. Granetz, A. Hubbard, J. A. Snipes, T. Sunn Pedersen, M. Greenwald, B. LaBombard, and the Alcator Group, *Plasma Phys. Control. Fusion* **41**, A609 (1999).
- ²ASDEX Team, *Nucl. Fusion* **29**, 1959 (1989).
- ³M. J. Greenwald, D. A. Gwinn, S. Milora et al., *Phys. Rev. Lett.* **53**, 352 (1984).
- ⁴E. S. Marmor, J. L. Terry, B. Lipschultz, and J. E. Rice, *Rev. Sci. Instrum* **60**, 3379 (1989).
- ⁵F. M. Levinton, M. C. Zarnstorff, S. H. Batha, M. Bell, R. E. Bell, R. V. Budny, C. Bush, Z. Chang, E. Fredrickson, A. Janos, J. Manickam, A. Ramsey, S. A. Sabbagh, G. L. Schmidt, E. J. Synakowski, and G. Taylor, *Phys. Rev. Lett.* **75**, 4417 (1995).
- ⁶E. J. Strait, L. L. Lao, M. E. Mauel, *et al.*, *Phys. Rev. Lett.* **75**, 4421 (1995).
- ⁷T. Fujita, S. Idei, H. Shirai *et al.*, *Phys. Rev. Lett.* **78**, 2377 (1997).
- ⁸O. Gruber, R. C. Wolf, R. Dux, *et al.*, *Phys. Rev. Lett.*, **83**, 1787 (1999).
- ⁹Y. Koide, M. Kikuchi, M. Mori, *et al.*, *Phys. Rev. Lett.* **72**, 3662 (1994).
- ¹⁰A. Fujisawa, H. Iguchi, T. Minami *et al.*, *Phys. Rev. Lett.* **82**, 2669 (1999).
- ¹¹B. LeBlanc, S. Batha, R. Bell *et al.*, *Phys. Plasmas* **2**, 741 (1995).
- ¹²S. I. Lashkul, V. N. Budnikov, A.A. Borevich, *et al.*, *Plasma Phys. Control. Fusion* **42**, A169 (2000).
- ¹³E. J. Doyle, G. M. Staebler, L. Zeng, T.L. Rhodes, K. H. Burrell, C. M. Greenfield, R. J. Groebner, G. R. McKee, W. A. Peebles, C. L. Rettig, B. W. Rice, and B. W. Stallard, *Plasma Phys. Controlled Fusion* **42**, A237 (2000).

- ¹⁴D. T. Garnier, E. S. Marmor, C. L. Fiore *et al.*, Proceedings of the 16th International Conference on Fusion Energy, Montreal, 1996, (IAEA, Vienna, 1997), Vol. I, 907.
- ¹⁵Y. Takase, R. Boivin, F. Bombarda, et al., in *Proceedings of the 16th International Fusion Energy Conference, Montreal, 1996* (International Atomic Energy Agency, Vienna, 1997), Vol. I, p. 475.
- ¹⁶H. Zohm, Plasma Phys. Controlled Fusion **38**, 105 (1996).
- ¹⁷M. Greenwald, R. Boivin, P. Bonoli *et al.*, Phys. Plasmas **6**, 1943 (1999).
- ¹⁸A. Hubbard, R. L. Boivin, R. S. Granetz *et al.*, Phys. Plasmas **5**, 1744 (1997).
- ¹⁹E. S. Marmor, R. L. Boivin, R. S. Granetz, J. W. Hughes, B. Lipschultz, S. McCool, D. Mossessian, C. S. Pitcher, J. E. Rice, and J. L. Terry, to be published, Rev. Sci. Instrum.
- ²⁰J. E. Rice and E. S. Marmor, Rev. Sci. Instrum. **66**, 752 (1995).
- ²¹J. E. Rice, P. T. Bonoli, J. A. Goetz et al., Nucl. Fusion **39**, 1175 (1999).
- ²²I. H. Hutchinson, J. E. Rice, J. A. Snipes, and R. S. Granetz, Phys. Rev. Lett. **84**, 3330 (2000).
- ²³C. L. Fiore and R. L. Boivin, Rev. Sci. Instrum. **66**, 945 (1995).
- ²⁴J. E. Rice, R. L. Boivin, P. T. Bonoli, "Observations of Toroidal Rotation Suppression with ITB Formation in ICRF and Ohmic H-mode Alcator C-Mod Plasmas", submitted to Nucl. Fusion.
- ²⁵Hawryluk, R., in Physics of Plasma Close to Thermonuclear Conditions, (Varenna, 1979), Commission of the European Communities, Brussels, Vol. I, p. 61 (1979).
- ²⁶G. M. Staebler, R. E. Waltz, J. C. Wiley, Nucl. Fusion **37**, 287 (1997).

Figure Captions

Figure 1. Density profiles at select points in time are shown for 4 Alcator C-Mod shots which demonstrated internal transport barrier formation: a.) At the H- to L-mode transition; b.) During lithium pellet injection; c.) With off-axis ICRF power injected on the high field side; d.) During a peaked density ohmic H-mode.

Figure 2. Central toroidal rotation and density peaking factor are compared for two similar discharges. The dashed line has the ICRF resonance at $r/a=0.25$ on the high field side, while the solid line represents the case where the ICRF resonance layer is at $r/a=0.5$ on the high field side. The ICRF input power was 3 MW, and it was turned on at 0.7 s in both cases.

Figure 3. Typical H- to L-mode transition are shown: neutron rate, central ion temperature, line average density, density peaking factor, and D_α emission.

Figure 4. The scale length ratio r/L_n and the global neutron rate are shown during an H- to L-mode transition.

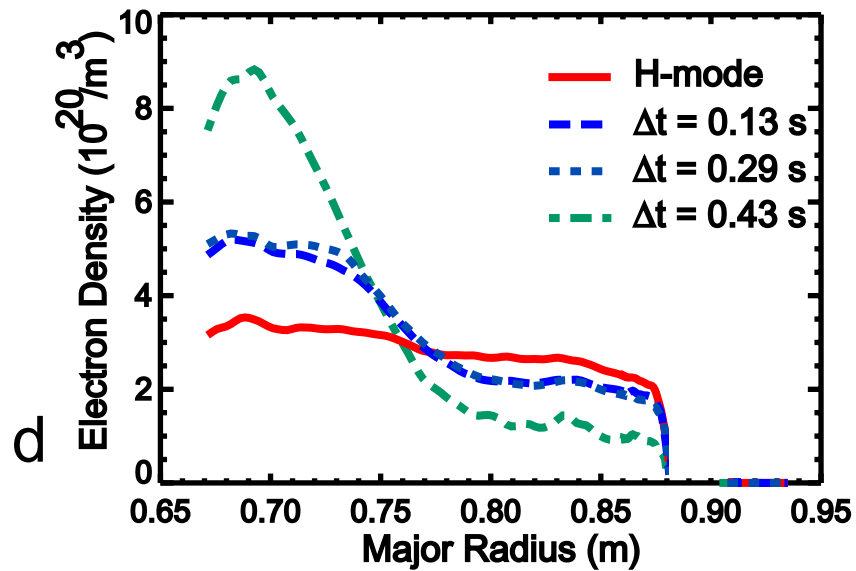
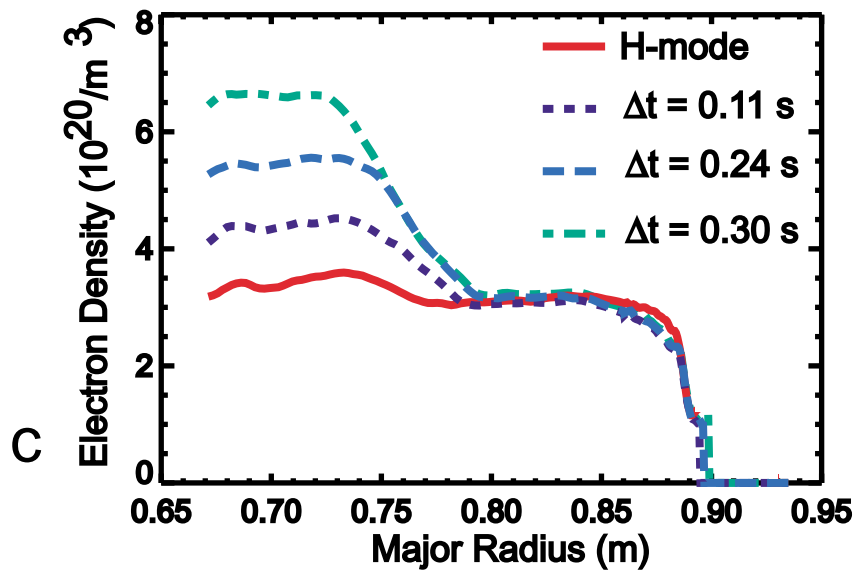
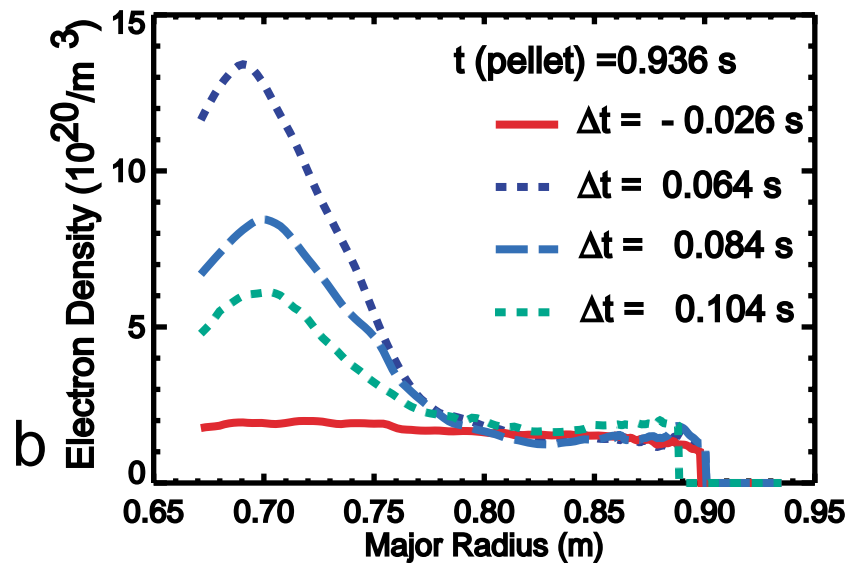
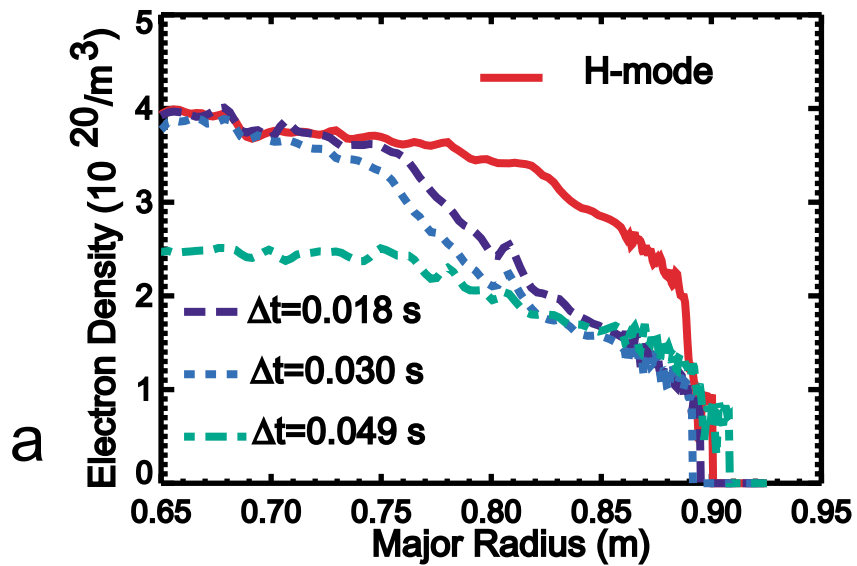
Figure 5. Ion temperature profiles obtained from Doppler broadened x-ray emission from argon impurity ions are provided before and during the H- to L- mode transition with the corresponding

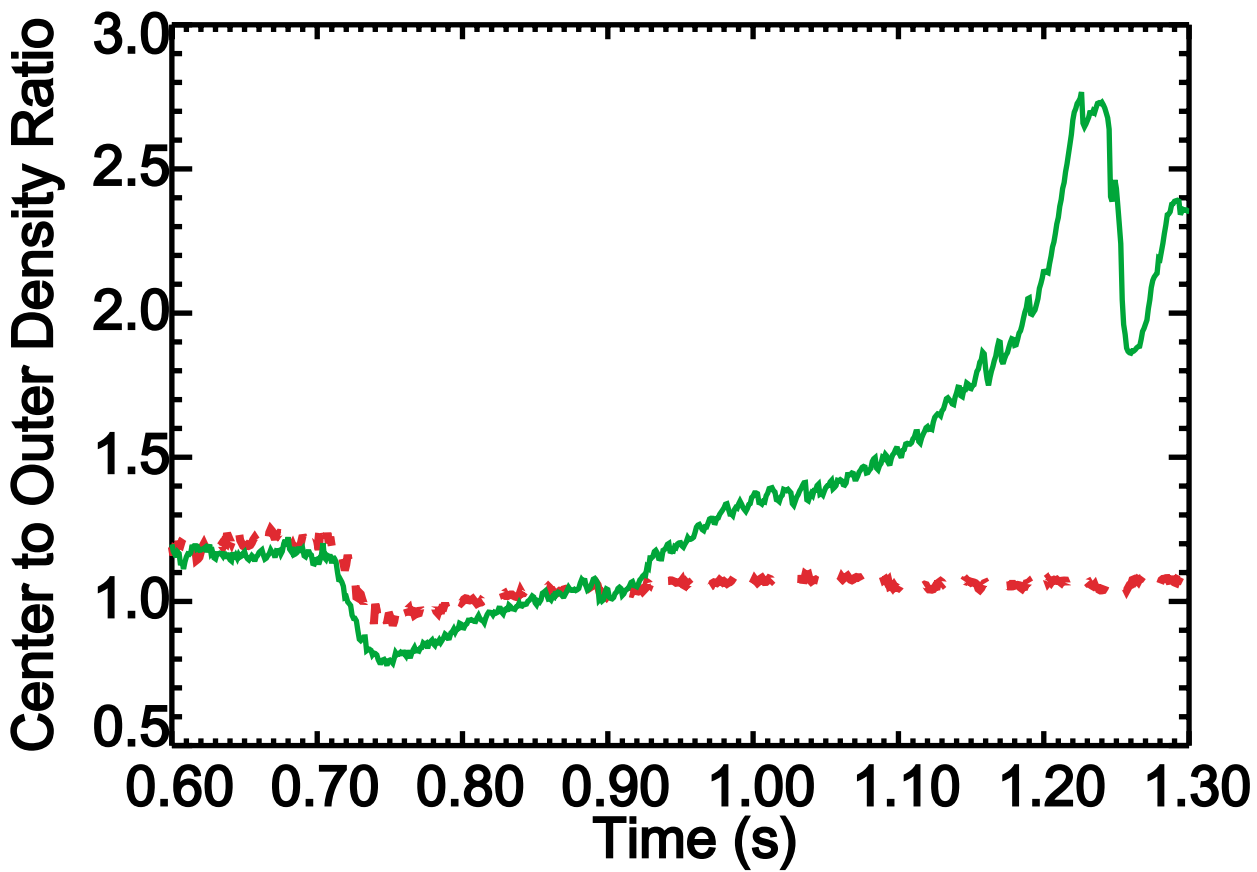
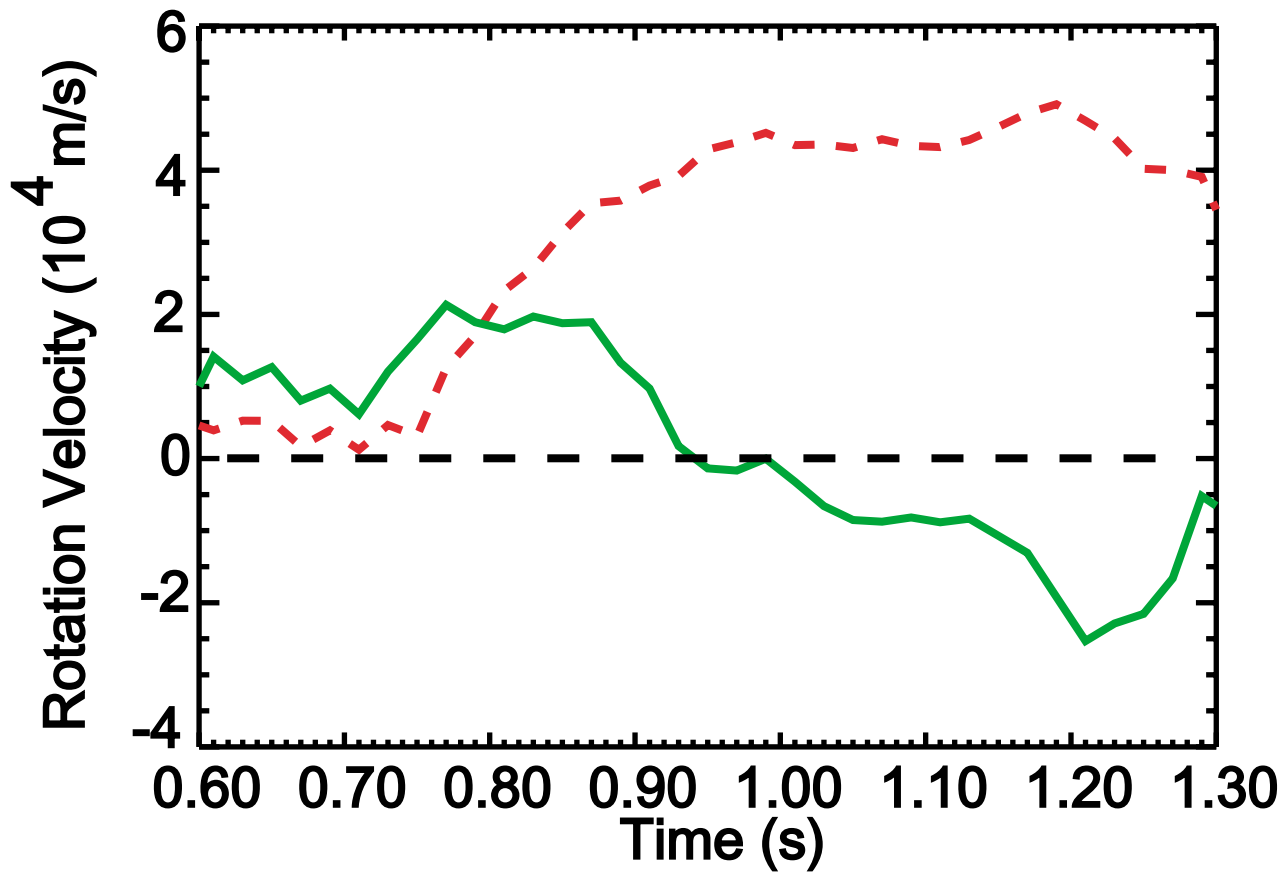
ion temperature obtained from inversion of the neutron and also the electron temperature profiles.

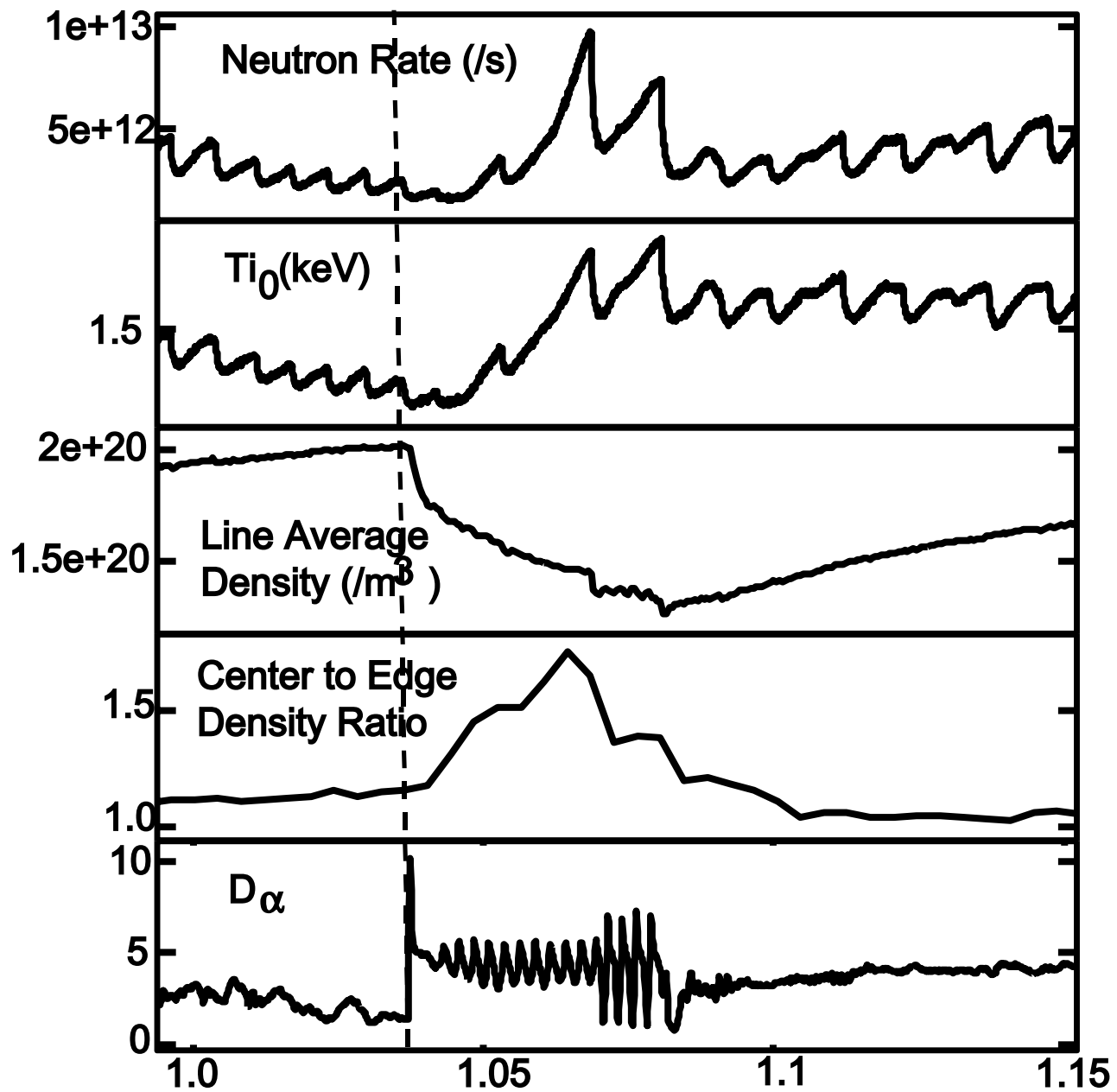
Figure 6. (a) The quantity η_e defined as $(d \ln (T_e)/dr) / d \ln (n_e)/dr$ is plotted during an H- to L-mode transition with the global neutron rate and (b) a histogram of the minimum value of η_e .

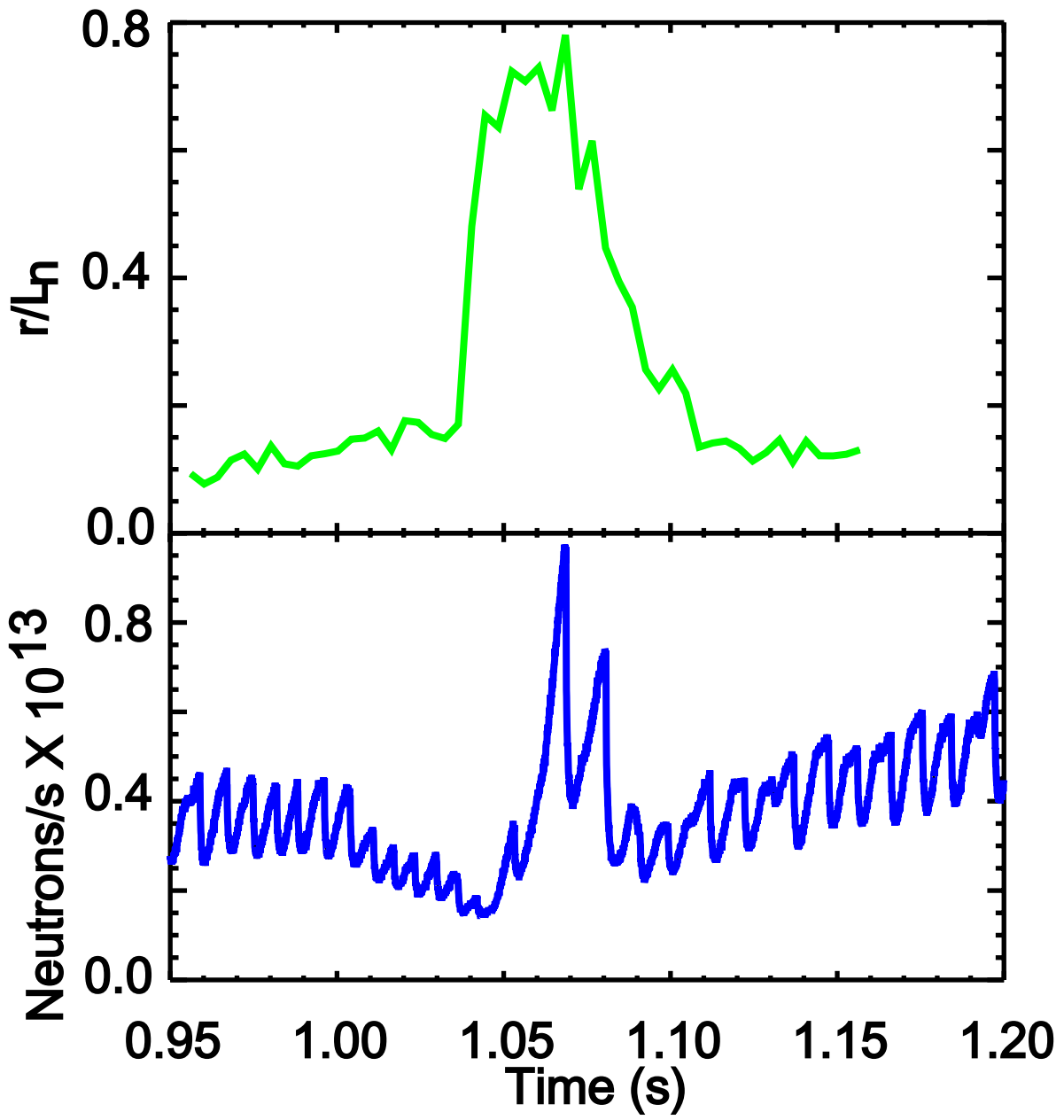
Figure 7. The neutron rate, central toroidal rotation velocity, line average density, density peaking factor are compared to TRANSP calculation of the total energy confinement time and the effective thermal diffusivity χ_{eff} at $r/a=0.3$. The H-mode terminates at 1.09 s.

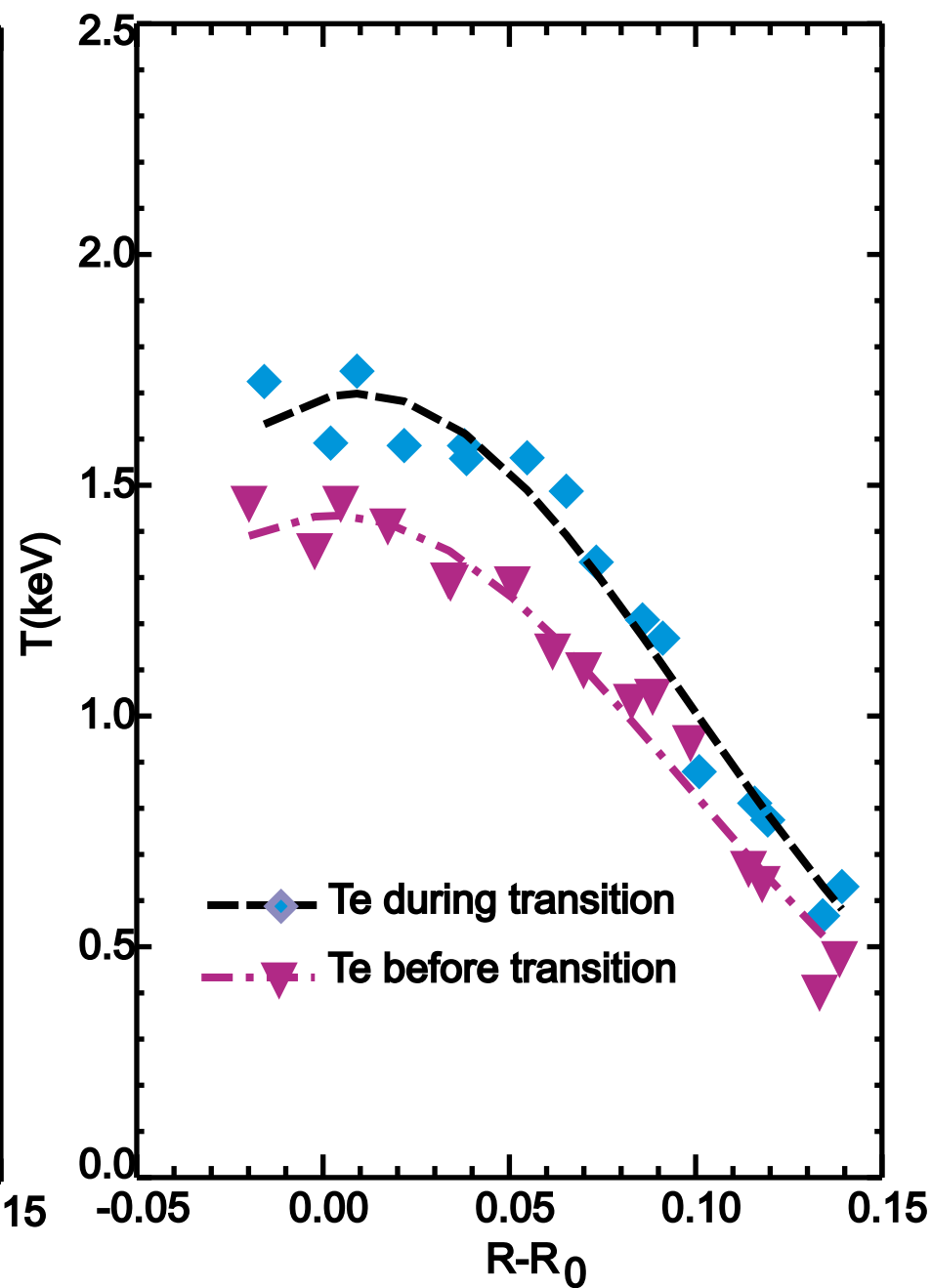
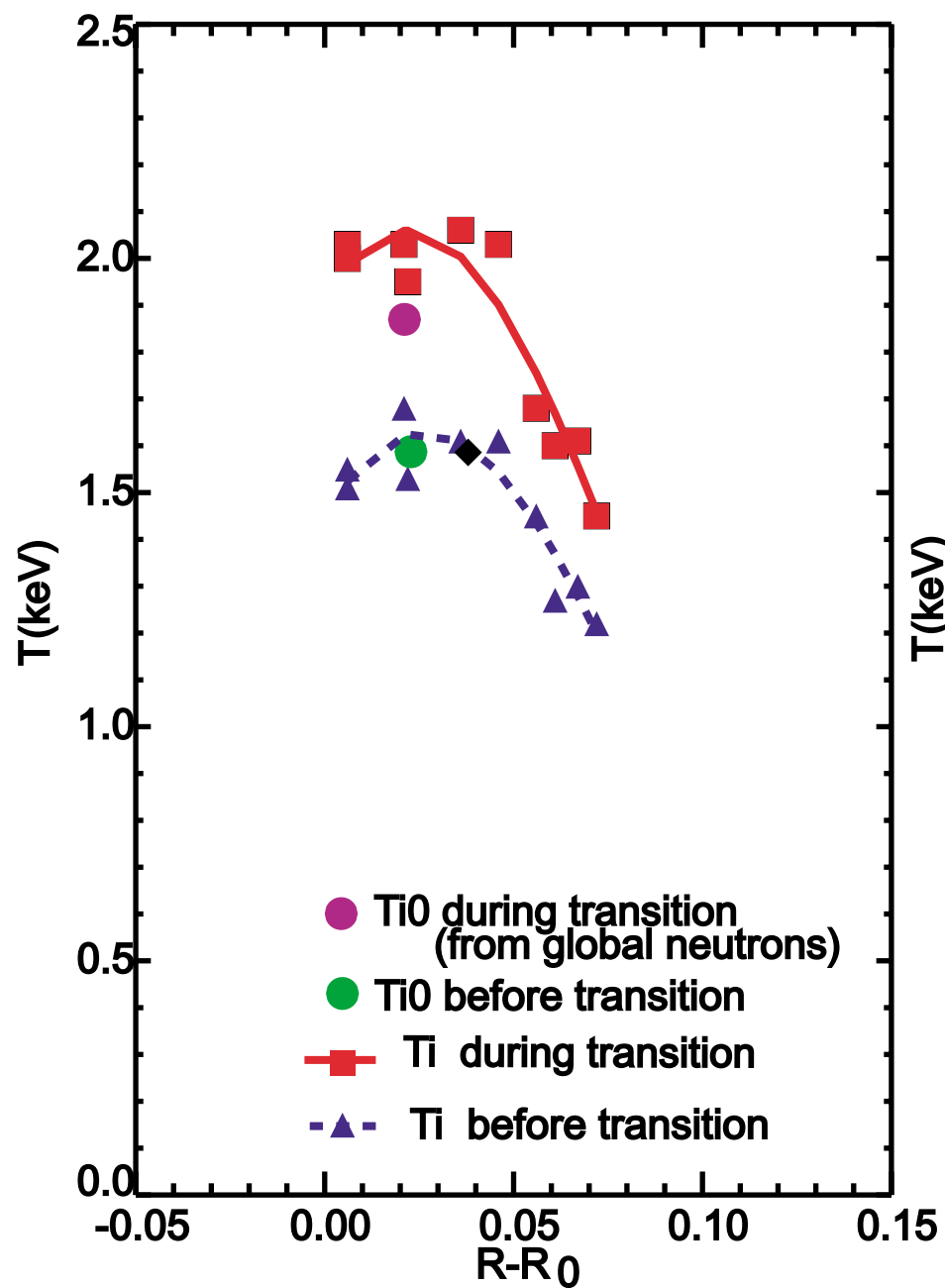
Figure 8. Radial profiles of the effective thermal diffusivity χ_{eff} , the energy confinement time and the bootstrap current density are shown, as determined by TRANSP for the ohmic H-mode plasma featured in Fig. 8.

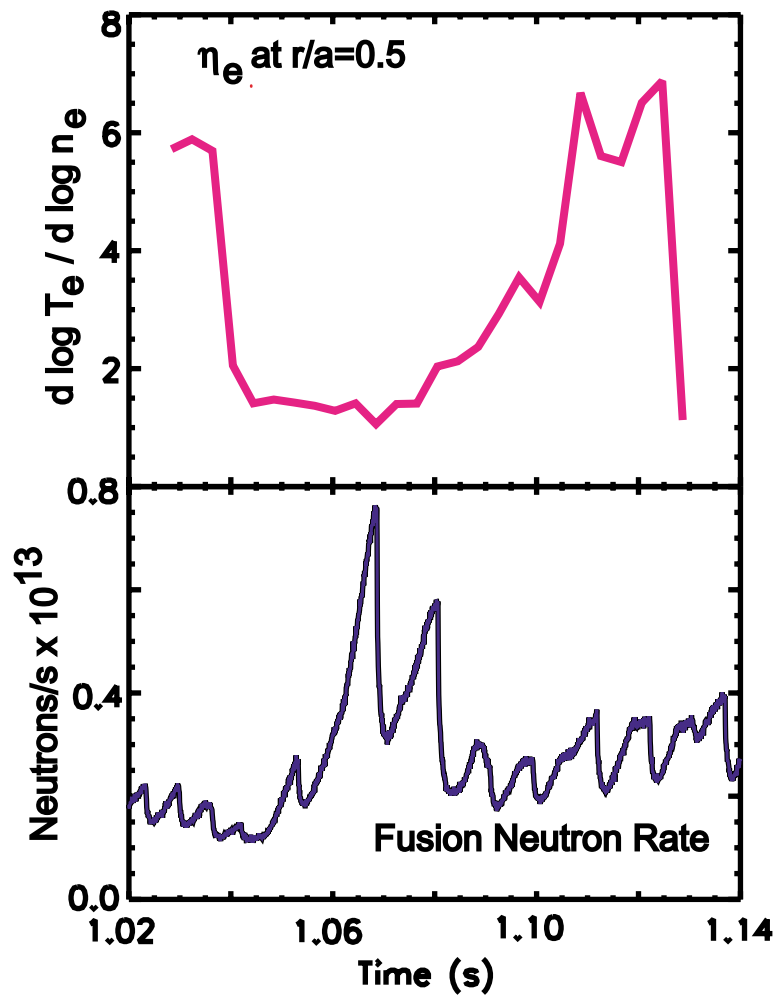




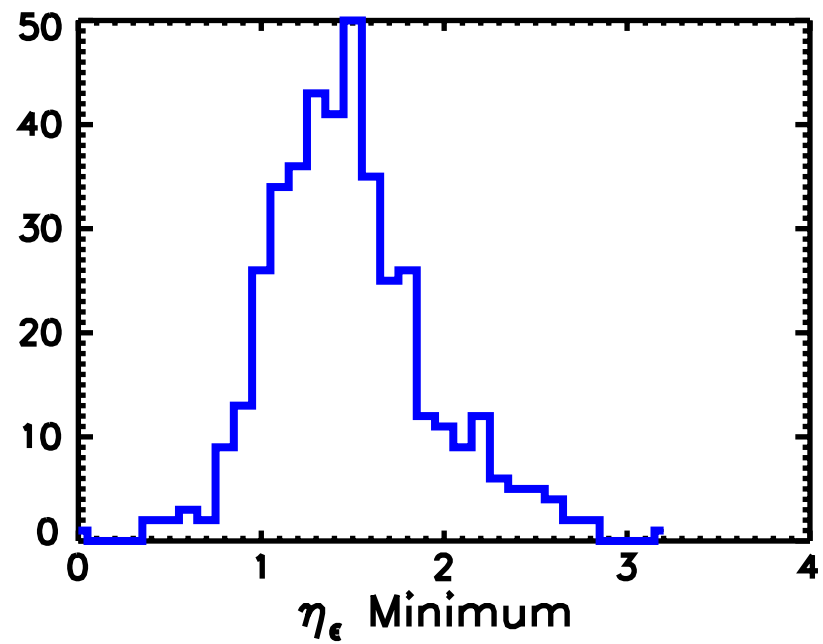








a



b

